Antitumor Effects of Chimeric Receptor Engineered Human T Cells Directed to Tumor Stroma

Sunitha Kakarla[1,2,3], Kevin KH Chow[1,2,3], Melinda Mata[1,2,4], Donald R Shaffer[1,2,3], Xiao-Tong Song[1,4], Meng-Fen Wu[5], Hao Liu[5], Lisa L Wang[2,6], David R Rowley[7], Klaus Pfizenmaier[8] and Stephen Gottschalk[1,2,3,4,6]

[1]Center for Cell and Gene Therapy, Texas Children's Hospital, The Methodist Hospital, Baylor College of Medicine, Houston, Texas, USA; [2]Texas Children's Cancer Center, Texas Children's Hospital, Baylor College of Medicine, Houston, Texas, USA; [3]Interdepartmental Program in Translational Biology and Molecular Medicine, Baylor College of Medicine, Houston, Texas, USA; [4]Department of Pathology and Immunology, Baylor College of Medicine, Houston, Texas, USA; [5]Biostatistics Shared Resource Dan L Duncan Center, Baylor College of Medicine, Houston, Texas, USA; [6]Department of Pediatrics, Baylor College of Medicine, Houston, Texas, USA; [7]Department of Molecular and Cellular Biology, Baylor College of Medicine, Houston, Texas, USA; [8]Institute of Cell Biology and Immunology, University of Stuttgart, Stuttgart, Germany

Cancer-associated fibroblasts (CAFs), the principle component of the tumor-associated stroma, form a highly protumorigenic and immunosuppressive microenvironment that mediates therapeutic resistance. Co-targeting CAFs in addition to cancer cells may therefore augment the antitumor response. Fibroblast activation protein-α (FAP), a type 2 dipeptidyl peptidase, is expressed on CAFs in a majority of solid tumors making it an attractive immunotherapeutic target. To target FAP-positive CAFs in the tumor-associated stroma, we genetically modified T cells to express a FAP-specific chimeric antigen receptor (CAR). The resulting FAP-specific T cells recognized and killed FAP-positive target cells as determined by pro-inflammatory cytokine release and target cell lysis. In an established A549 lung cancer model, adoptive transfer of FAP-specific T cells significantly reduced FAP-positive stromal cells, with a concomitant decrease in tumor growth. Combining these FAP-specific T cells with T cells that targeted the EphA2 antigen on the A549 cancer cells themselves significantly enhanced overall antitumor activity and conferred a survival advantage compared to either alone. Our study underscores the value of co-targeting both CAFs and cancer cells to increase the benefits of T-cell immunotherapy for solid tumors.

Received 8 November 2012; accepted 1 April 2013; advance online publication 4 June 2013. doi:10.1038/mt.2013.110

INTRODUCTION

The tumor-associated stroma has garnered increasing attention for its role in initiating and sustaining tumor growth. Occupying up to 90% of the tumor mass,[1] the stroma is composed of heterogeneous cell types, of which cancer-associated fibroblasts (CAFs) are preponderant.[2] CAFs support tumor progression directly through paracrine secretion of cytokines, growth factors and so on,[3] and indirectly by mediating resistance to chemotherapy, radiotherapy, and immunotherapy.[4,5] Additionally, therapies directed to cancer cells often fail to eradicate CAFs, which can reinstate a tumorigenic milieu and favor recurrence.[6,7]

It is now evident that CAFs express markers that distinguish them from their normal counterparts,[8] allowing them to be selectively targeted. One such marker is fibroblast activation protein-α (FAP), a type 2 dipeptidyl peptidase originally isolated from CAFs in human sarcomas.[9] FAP expression was subsequently detected on cancer-associated fibroblasts in over 90% of common epithelial cancers including colorectal, breast, pancreatic, skin, and lung[10] tumors, and is often correlated with poor prognosis.[11] Selective ablation of FAP-positive stromal cells in a transgenic mouse model permitted immunological control of tumor growth, indicating their significant immunosuppressive function in the microenvironment.[12] Targeting FAP-positive cancer-associated fibroblasts therefore presents an attractive strategy to augment current immunotherapies. While several groups have evaluated the use of FAP-targeted vaccines,[13] no study so far has determined whether the adoptive transfer of FAP-specific T cells enhances current T-cell therapy approaches for solid tumors.

Here we report the development of a FAP-specific chimeric antigen receptor (CAR) to redirect T cells to FAP-positive cancer-associated fibroblasts. These T cells recognize and kill FAP-positive targets *in vitro* and suppress tumor growth in both loco-regional and systemic tumor models. When combined with CAR-T cells targeting a tumor-associated antigen, they significantly enhanced antitumor effects in comparison to animals treated with FAP- or tumor-specific T cells alone.

RESULTS

Generation of FAP-specific CAR modified T cells

We generated a second generation CAR specific for both murine and human FAP (mhFAP) using the single chain variable

Correspondence: Stephen Gottschalk, Center for Cell and Gene Therapy, Baylor College of Medicine, 1102 Bates Street, Suite 1770, Houston, TX 77030, USA. E-mail: smgottsc@txch.org

fragment scFV MO36 (mhFAP-CAR; **Figure 1a**).[14,15] T cells were transduced with a retroviral vector encoding the mhFAP-CAR to generate FAP-specific T cells. Five days after transduction, CAR expression was measured by flow cytometry using a CH2CH3 antibody. Over 75% of the T cells were CAR positive ($n = 5$; range 57.7–90.5%; **Figure 1b**) and contained both CD4-positive and CD8-positive T-cell populations.

FAP-specific T cells recognize and kill both human and murine FAP-positive targets

To investigate the functionality of FAP-specific T cells, we used qRT-PCR amplification and/or FACS analysis to measure the expression of human FAP by a panel of cell lines, including the metastatic lung fibroblast cell line (Hs894), prostate cancer-associated fibroblast cell line HPS-19I,[16] melanoma (SENMA), nasopharyngeal carcinoma (C666.1), glioblastoma (U87), pancreatic ductal carcinoma (PL45), lung cancer (A549) and lymphoblastoid cells (LCLs). All lines expressed FAP except for A549 and LCLs (**Figure 2a**,**b**). To demonstrate FAP-specific recognition of target cells, we first transduced FAP-negative A549 cells with a lentiviral vector encoding either murine or human FAP (A549.mFAP or A549.hFAP; **Figure 2a**,**b**). We co-cultured tumor cells with FAP-specific T cells or nontransduced (NT) T cells for 24 hours and measured proinflammatory cytokines in the cell culture supernatants by Multiplex analysis. FAP-specific T cells recognized both murine (A549.mFAP) and human (A549.hFAP) cell lines as evidenced by the release of proinflammatory cytokines such as IFNγ and TNFα with no release on exposure to FAP-negative A549 target cells ($P < 0.05$). While FAP-specific T cells also secreted IL-6 and IL-13, they did not secrete significant amounts of GM-CSF, IL-2, IL-4, IL-5, IL-7, or IL-8. Similarly, NT-T cells produced little to no proinflammatory cytokines in response to either FAP-positive or FAP-negative target cells (**Figure 2c**, **Supplementary Figure S1**). In a standard ^{51}Cr release assay, FAP-specific T cells had significant cytotoxic activity against A549.mFAP and A549.hFAP, whereas NT-T cells did not ($P = 0.0005$; **Figure 2d**). To provide additional evidence that the expression of FAP-CARs is critical for the observed effect, we performed a cytotoxicity assay using T cells expressing a prostate stem cell antigen (PSCA)-specific CAR.[17] While PSCA-specific T cells killed PSCA-transduced K562 cells, PSCA-specific T cells did not kill parental A549 cells or A549 cells-transduced with murine or human FAP (**Figure 2e**). Hence, T-cell recognition depends on the expression of FAP-specific CARs by T cells and the presence of murine or human FAP on target cells.

We confirmed the above findings by using a range of FAP-positive and FAP-negative tumor cell lines. FAP-specific T cells secreted significantly more IFNγ ($P < 0.05$) and TNFα ($P < 0.05$) than NT-T cells in co-culture assays with FAP-positive cells (SEMNA, U87, Hs894, and HPS-19I) but not with FAP-negative cells (LCL and A549; **Figure 3a**,**b**). FAP-specific T cells also killed FAP-positive (SENMA, U87, Hs894, and HPS-19I; $P < 0.05$) but not FAP-negative (LCL, A549) target cells in a standard ^{51}Cr release assays (**Figure 3c**). NT-T cells showed little to no cytolytic activity. Thus FAP-specific T cells recognize and kill targets that naturally express FAP.

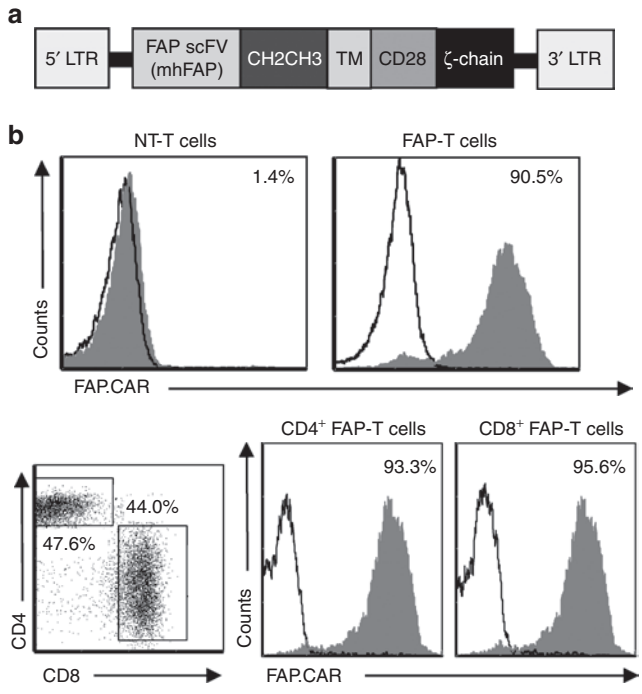

Figure 1 Generation of FAP-specific T cells. (**a**) Schematic of the FAP-specific CAR retroviral vector. (**b**) Representative data from one donor showing CAR expression and T-cell subsets.

FAP-specific T cells have antitumor activity in a loco-regional tumor model

To assess the effects of targeting FAP-positive cancer-associated fibroblasts in the tumor-associated stroma, we first used a loco-regional tumor model with FAP-negative LCLs. We tracked tumor growth *in vivo* by serial bioluminescence imaging of modified LCLs expressing a GFP firefly luciferase fusion protein (LCL.eGFP.ffLuc).[18] To determine if LCL.eGFP.ffLuc induced FAP-positive reactive stroma *in vivo*, we injected severe combined immunodeficiency (SCID) mice subcutaneously (s.c.) with 5×10^6 LCL.eGFP.ffLuc cells, euthanized them at different time points post tumor injection, and quantified murine FAP in the tumors by qRT-PCR amplification. FAP expression was detected when measured three days post tumor cell injection (**Figure 4a**). The presence of reactive stroma was confirmed by immunohistochemistry for smooth muscle α-actin and immunofluorescence staining for FAP (**Supplementary Figure S2**).

To investigate the effects of targeting FAP-positive reactive stroma on tumor growth, we injected subcutaneously an admixture of 5×10^6 LCL.eGFP.ffLuc cells and 10×10^6 FAP-specific T cells or nontransduced T cells ($n = 10$). Bioluminescence imaging showed that FAP-specific T cells significantly decreased tumor growth compared to mice receiving NT-T cells ($P = 0.003$ on day 4; $P = 0.0003$ on day 8; $P = 0.002$ on day 11, and $P = 0.01$ on day 14; **Figure 4b**,**c**). To exclude *in vivo* induction of FAP expression on LCL tumor cells themselves, we generated a second FAP-specific CAR that only recognizes human FAP (hFAP-CAR, **Supplementary Figure S3**) and would therefore not be reactive against the mFAP present on the murine stroma. hFAP-specific T cells had no significant antitumor activity when injected with LCL.eGFP.ffLuc cells at any time point ($P = 0.43$ on day 4; $P = 0.64$ on day 8; $P = 0.35$ on day 11, and $P = 0.17$ on day 14; **Supplementary Figure S4a,b**). Hence, induction

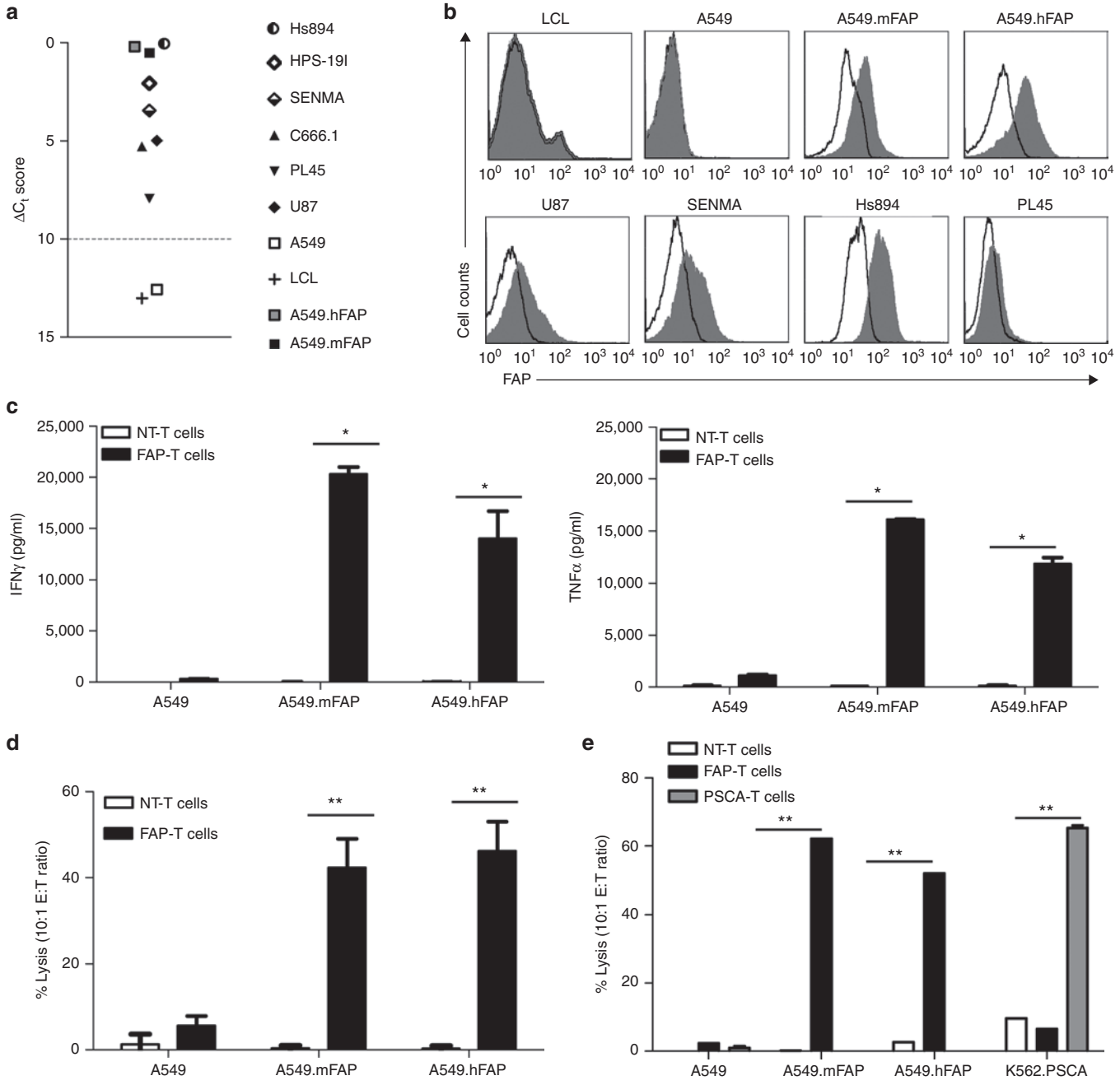

Figure 2 FAP-specific T cells recognize and kill human or murine FAP-positive cells. (**a**) qRT-PCR. (**b**) FACS analysis on a panel of cancer cell lines and cancer-associated fibroblast cell lines using human FAP primers. (**c**) NT- or FAP-T cells were co-cultured with FAP$^+$ target cells (A549.mFAP, A549.hFAP) and FAP$^-$ targets (A549) at a 2:1 effector: target (E:T) ratio. The production of proinflammatory cytokines IFN-γ and TNF-α by T cells was determined by Milliplex MAP after 24 hr ($n = 4$ independent replicates; means + SD). (**d**,**e**) FAP-, PSCA-, and NT-T cells were tested in standard 6-hr chromium release assays at 10:1 E:T ratio ($n = 5$; mean + SD). *$P < 0.05$; **$P < 0.005$.

of human FAP on tumor cells cannot explain the benefit of FAP-specific T cells in this xenograft model and the observed antitumor activity depends instead on the presence of T cells that recognize and target murine FAP.

FAP-specific T cells have antitumor activity in a systemic tumor model

We next measured the effects of stroma targeting with FAP-specific T cells in a systemic rather than a loco-regional tumor model. We used an A549 lung cancer model since cancer-associated fibroblasts play an important role in lung cancer development[19] and A549 cells are negative for FAP expression. We generated an A549.eGFP.ffLuc cell line to allow noninvasive bioluminescence imaging. To assess if A549 cells induce FAP-positive stroma *in vivo*, we injected 2.5×10^6 A549.eGFP.ffLuc cells into the tail vein of SCID-Beige (SCID-Bg) mice. Mice were then euthanized at different time points and mFAP in the lungs quantified by qRT-PCR analysis. mFAP expression was detected when measured on day 4-post

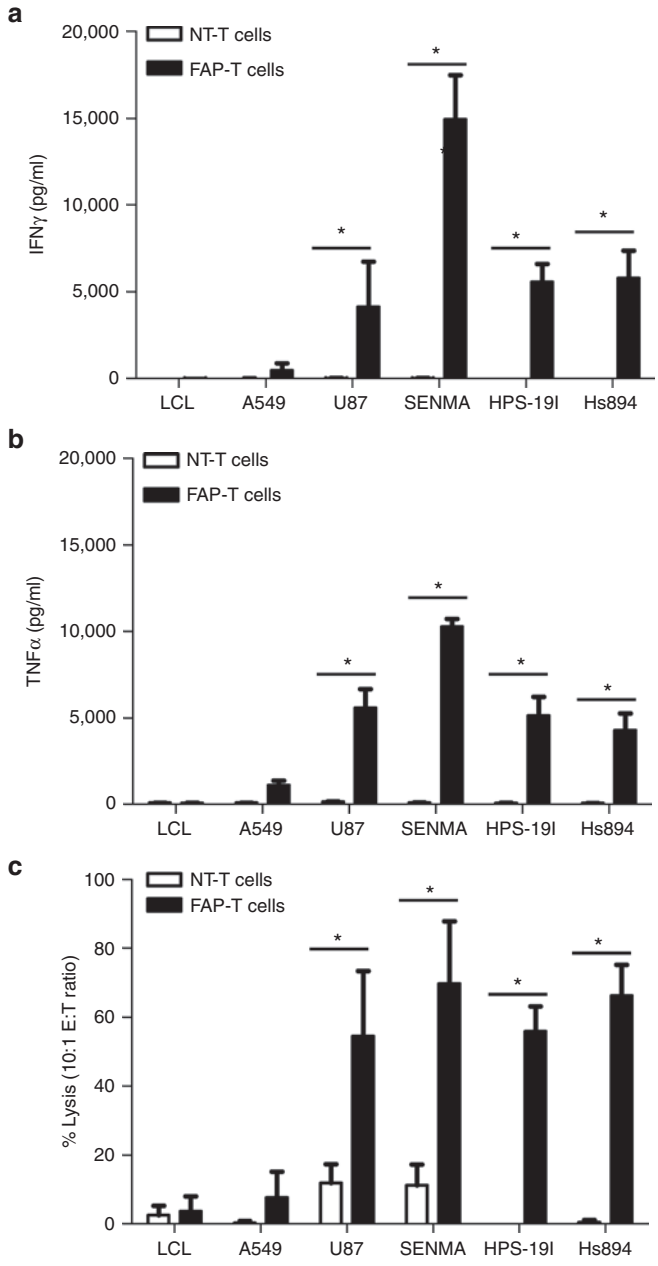

Figure 3 FAP-specific T cells recognize and kill cells expressing FAP from its endogenous promoter. (**a**) NT- or FAP-T cells were co-cultured with FAP$^+$ target cells (U87, SENMA, HPS-19I, and Hs894) and FAP$^-$ (LCL and A549) at a 2:1 effector: target (E:T) ratio. (**b**) The production of IFN-γ and TNF-α by T cells was determined by Milliplex MAP after 24 hr (n = 3 independent replicates; mean ± SD). (**c**) FAP- and NT-T cells were tested in standard 6-hr chromium release assays at 10:1 E:T ratio (n = 3 independent replicates; mean ± SD). *P < 0.05.

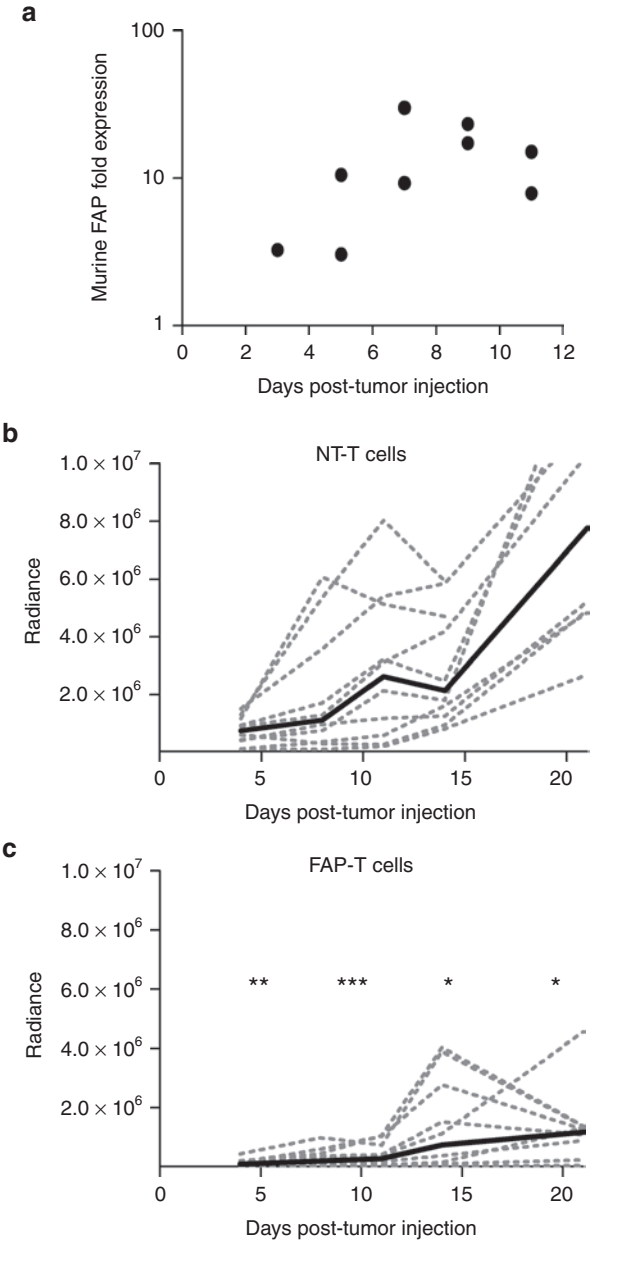

Figure 4 FAP-specific T cells suppress LCL tumor growth. (**a**) Induction of murine FAP expression *in vivo*. Relative fold expression ($2^{-\Delta\Delta C_t}$) was quantified in comparison to normal skin using murine FAP primers. Each dot represents a single tumor sample from different mice at each time point. (**b**) An admixture of LCL.eGFP.FFLuc cells and NT-T cells. (**c**) FAP-T cells were injected subcutaneously along with 1,500 U of IL-2 administered i.p. (n = 10/group) on day 0. Bioluminescence signal (radiance = photons/sec/cm^2/sr) was monitored over time. *P < 0.05; **P < 0.005; ***P < 0.0005.

tumor cell injection (Figure 5a). Immunohistochemical analysis of lungs excised on day 11 post tumor cell injection showed tumors with FAP-positive stroma. No such stroma was present in control mice (**Supplementary Figure S5**).

To evaluate the antitumor effects of targeting FAP-positive cells, 2.5×10^6 A549.eGFP.ffLuc cells were injected intravenously into SCID-Bg mice on day 0. On day 4, 10×10^6 FAP-specific T cells or NT-T cells were administered intravenously in conjunction with an intraperitoneal injection of rhIL-2 (1,500 U). A total of three doses of T cells and IL-2 were administered at weekly intervals. Untreated mice served as controls. Quantification of bioluminescent imaging showed exponential tumor growth in control mice receiving NT-T cells, while mice receiving FAP-specific T cells had a significant decrease in tumor growth (FAP vs. Untreated P < 0.0001, FAP vs. NT P = 0.0012 on day 20; Figure 5b–e). Moreover, FAP-specific T cells significantly prolonged survival of mice compared with the

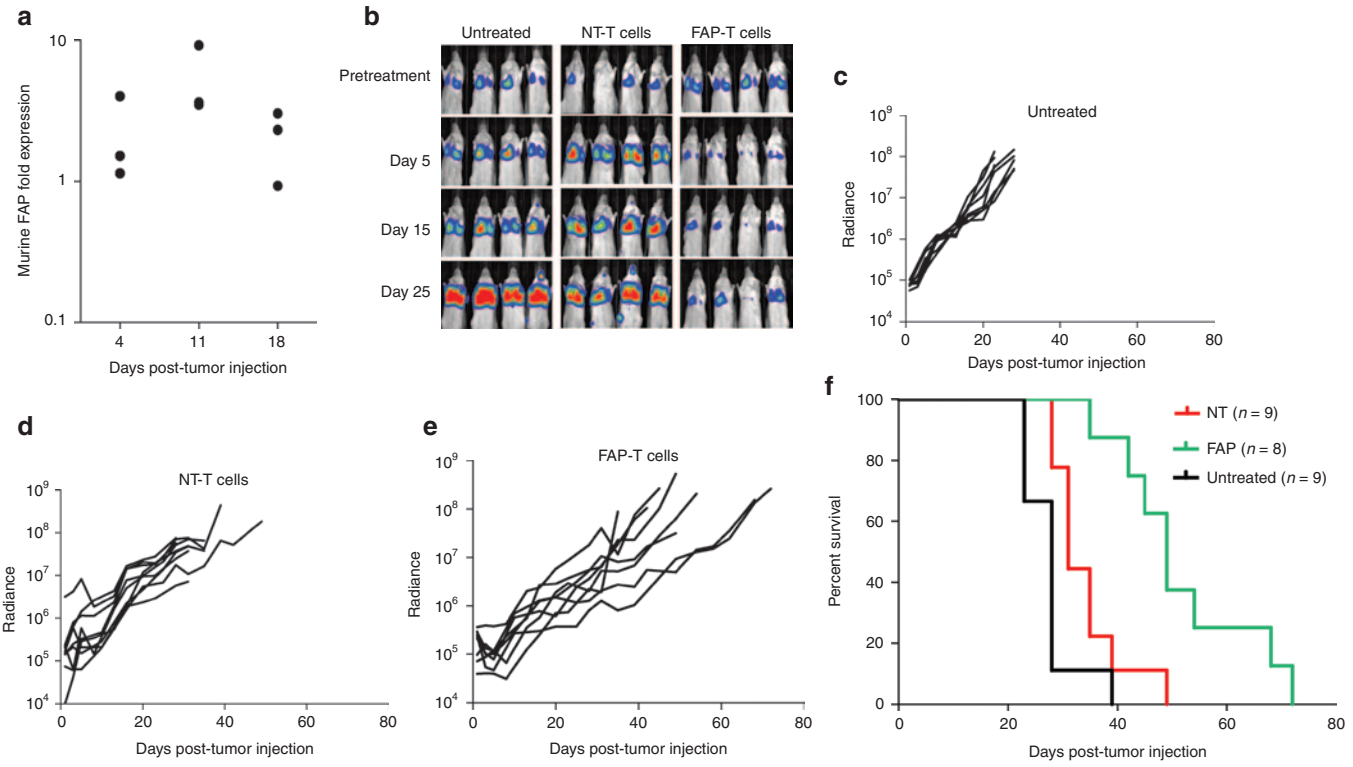

Figure 5 FAP-specific T cells decrease tumor growth and improve survival in an A549 lung cancer model. (**a**) A549.eGFP.FFLuc cells were injected i.v. Lungs were excised and qRT-PCR was used to determine relative levels of murine FAP expression in the lungs using murine FAP primers. Relative fold expression (2^-ΔΔCt) was quantified in comparison to normal lungs. Each dot represents a single lung sample from different mice at each time point. (**b**) A549.eGFP.FFLuc cells were injected i.v. into mice on day 0 and treated i.v. with FAP-T cells and 1, 500 U IL-2 administered i.p. on day 4. Treatment was repeated two more times a week apart. Untreated mice and mice treated with NT-T cells served as controls. Tumor progression was followed by *in vivo* bioluminescence imaging. Images of representative animals are shown. (**c–e**) Solid lines represent each individual mouse. (**f**) Kaplan–Meier survival curve of untreated mice ($n = 9$) or those treated with FAP ($n = 8$) or NT-T cells ($n = 9$).

untreated cohort or those treated with NT-T cells ($P < 0.0001$; **Figure 5f**). Treatment with hFAP-specific T cells had no effects similar to the NT-control T cells (**Supplementary Figure S6**), indicating that the antitumor effect is a result of targeting mFAP-positive stroma.

To provide direct evidence that FAP-specific T cells kill mFAP-positive cancer-associated fibroblasts we injected mice intravenously with 2.5×10^6 A549.eGFP.ffLuc cells followed by FAP-specific or NT-T cells on day 4. mFAP expression in the lungs was determined 48 hours later. FAP-specific T cells significantly decreased mFAP expression in comparison to NT-T cells ($P = 0.0043$; **Figure 6a**). We then injected mice intravenously with 2.5×10^6 A549.eGFP.ffLuc cells, and on day 4 we excised the lungs and dissociated them to single cell suspensions. Cells were subsequently co-cultured with FAP-specific or NT-T cells for 72 hours before FACS analysis for GFP-positive cancer cells and GFP-negative/FAP-positive cancer-associated fibroblasts. FAP-specific T cells eliminated FAP-positive cancer-associated fibroblasts, while NT-T cells did not ($P < 0.05$; **Figure 6b,c**).

While mFAP-specific T cells inhibited tumor growth, the tumors eventually progressed. To discover if this escape is due to limited T-cell persistence, 2.5×10^6 A549 were injected intravenously into 15 mice on day 0. On day 4, 10×10^6 eGFP.ffLuc-expressing FAP-specific T cells (or) 10×10^6 eGFP.ffLuc-expressing hFAP-specific T cells (or) 10×10^6 eGFP.ffLuc-expressing NT-T cells were injected intravenously into mice (5 animals per group; **Supplementary Figure S7a**). Additionally, five nontumor bearing mice received 10×10^6 eGFP.ffLuc-expressing FAP-specific T cells as controls. All animals received an intraperitoneal injection of rhIL-2 (1,500 U). *In vivo* imaging system was used to follow T-cell persistence. FAP-specific T cells homed to lungs, where they expanded and persisted for one week. In contrast, hFAP-T cells and NT-T cells disappeared within 48 hours after administration as did FAP-specific T cells that were injected into nontumor bearing mice (**Supplementary Figure S7b**). Thus tumor progression is most likely due to limited T-cell persistence *in vivo*.

The *in vivo* experiments conducted so far demonstrated the antistromal activity of FAP-specific T cells in the absence of overt toxic effects. To provide additional safety data, tumor-bearing mice were injected on day 4 with 10×10^6 eGFP.ffLuc-expressing FAP-specific T cells. Forty-eight hours post injection mice were euthanized and lungs, bone marrow, spleen, liver, and kidneys were subjected to pathological analysis. Untreated mice ($n = 5$) served as controls. Pathological analysis revealed mixed inflammatory cells composed predominantly of neutrophils, infiltrating the perivascular and peribronchial sites of mice injected with FAP-specific T cells that were absent in untreated controls. No histological differences were seen in other tissues (**Supplementary Figure S8a**). Similarly, a skin wound healing assay performed one day prior to T-cell injection of tumor-bearing mice showed no difference between FAP-specific T cells and NT-T cells ($n = 5$; **Supplementary Figure S8b,c**).

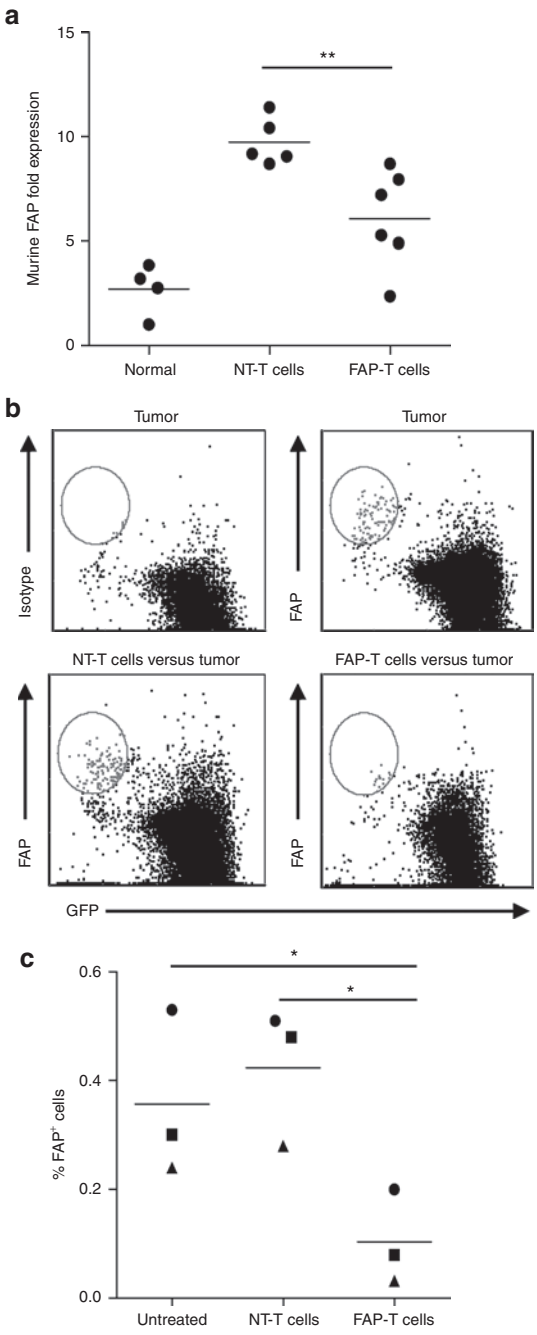

Figure 6 FAP-specific T cells recognize and kill murine FAP-positive stromal cells. (**a**) A549.eGFP.FFLuc were injected i.v. on day 0. On day 4 mice were treated with NT- or FAP-T cells administered i.v. along with 1,500 U IL-2 administered i.p. Lungs were excised 48 hr post treatment and relative fold expression (2^-ΔΔCt) was quantified in comparison to normal lungs by qRT-PCR using murine FAP primers. Data are means obtained from six lung specimens in each treatment group. Four normal lung specimens were used as control $^{**}P < 0.005$. (**b**) A549.eGFP.FFLuc cells were injected i.v. into SCID-Beige mice on day 0. Lungs were excised on day 4, dissociated to form single cell suspensions and co-cultured with NT- or FAP-T cells at 2:1 E:T ratio or left untreated. 72 hr later the presence of FAP-positive cells and GFP-positive tumor cells was determined by FACS analysis. Representative data for one such single cell suspension is shown. (**c**) Percentage FAP+ cells were determined for 25,000-gated events. Each symbol represents one lung specimen. $^{*}P < 0.05$.

Differential gene expression is induced in lungs of mice treated with FAP-specific T cells compared to NT-T cells

To explore the changes in the lung microenvironment associated with the antitumor response, we excised lungs from mice receiving FAP-specific or NT-T cells 48 hours post treatment. After affymetrix analysis ($n = 6$ replicates for each group) using mouse genome 1.0 ST arrays, we selected differentially expressed genes that were both ≥1.5-fold change from baseline and significantly different ($P < 0.05$) between the experimental (FAP-specific T cells) and control group (NT-T cells). About 277 genes were upregulated and 75 genes downregulated in mice treated with FAP-specific T cells compared to those receiving NT-T cells. Pathway analysis of the differentially expressed genes revealed enrichment of genes involved in chemokine and cytokine–cytokine receptor interaction ($P = 3.47 \times 10^{-8}$), toll-like receptor pathway ($P = 5.56 \times 10^{-5}$), natural killer cell mediated cytotoxicity ($P = 0.0001$), Jak-STAT pathway ($P = 0.0044$), B-cell receptor signaling ($P = 0.0266$), antigen processing and presentation pathway ($P = 0.0329$), complement and coagulation cascades ($P = 0.0238$), RIG-1-like signaling pathway ($P = 0.0238$), pathways in cancer ($P = 0.0382$day), type 2 interferon signaling ($P = 4.41 \times 10^{-8}$), IL-2 ($P = 0.0382$) and IL-3 receptor signaling ($P = 0.009$), and EGFR1 signaling pathway ($P = 0.0366$) as specified by Kyoto Encyclopedia of Genes and Genomes (KEGG) and wikipathways database (**Supplementary Table S1**).

Co-targeting cancer cells and CAFs results in enhanced antitumor effects

We next determined if the antitumor effects observed with FAP-specific T cells could be further enhanced by adding T cells directly targeted to the tumor cells themselves. We targeted the A549 tumor-associated antigen erythropoietin-producing hepatocellular carcinoma A2 (EphA2), which is also overexpressed by primary lung tumor cells.[20] T cells expressing an EphA2-specific CAR were generated as previously described.[21] EphA2-specific CAR was expressed by a median of 36.6% of vector-treated T cells (range 31.4–77.0%; $n = 5$; **Supplementary Figure S9a**). In functional assays, EphA2-specific T cells recognized and killed EphA2 positive targets (NCI-H1299, A549, and K562.hEphA2) but not EphA2-negative K562 cells (**Supplementary Figure S9b,c**). We injected 2.5×10^6 A549.eGFP.ffLuc cells intravenously into SCID-Bg mice, and then on day 7 we injected these animals intravenously with 10×10^6 FAP-specific T cells ($n = 5$), 10×10^6 EphA2-specific T cells ($n = 5$) or an admixture of 5×10^6 FAP-specific T cells and 5×10^6 EphA2-specific T cells ($n = 5$) along with one intraperitoneal injection of rhIL-2 (1,500 U). A total of three doses of T cells and IL-2 were administered at weekly intervals. We monitored tumor growth by bioluminescence imaging, and untreated mice served as the control. After four weeks, FAP- and EphA2-specific T cells had significant antitumor activity (FAP-T cells vs. untreated $P = 0.004$; EphA2-T cells vs. untreated $P = 0.0267$). However, the combination of FAP- and EphA2-specific T cells had the greatest antitumor activity (FAP-T cells + EphA2-T cells vs. FAP-T cells $P = 0.0002$; FAP-T cells + EphA2-T cells vs. EphA2-T cells $P = 0.0163$ on day 29; **Figure 7a–e**), sufficient to significantly increase the survival of mice receiving both FAP-specific and EphA2-specific T cells ($P < 0.0001$, **Figure 7f**). These mice did however eventually succumb to the disease. To evaluate if recurrent tumors consisted of antigen loss variants, the tumors were excised

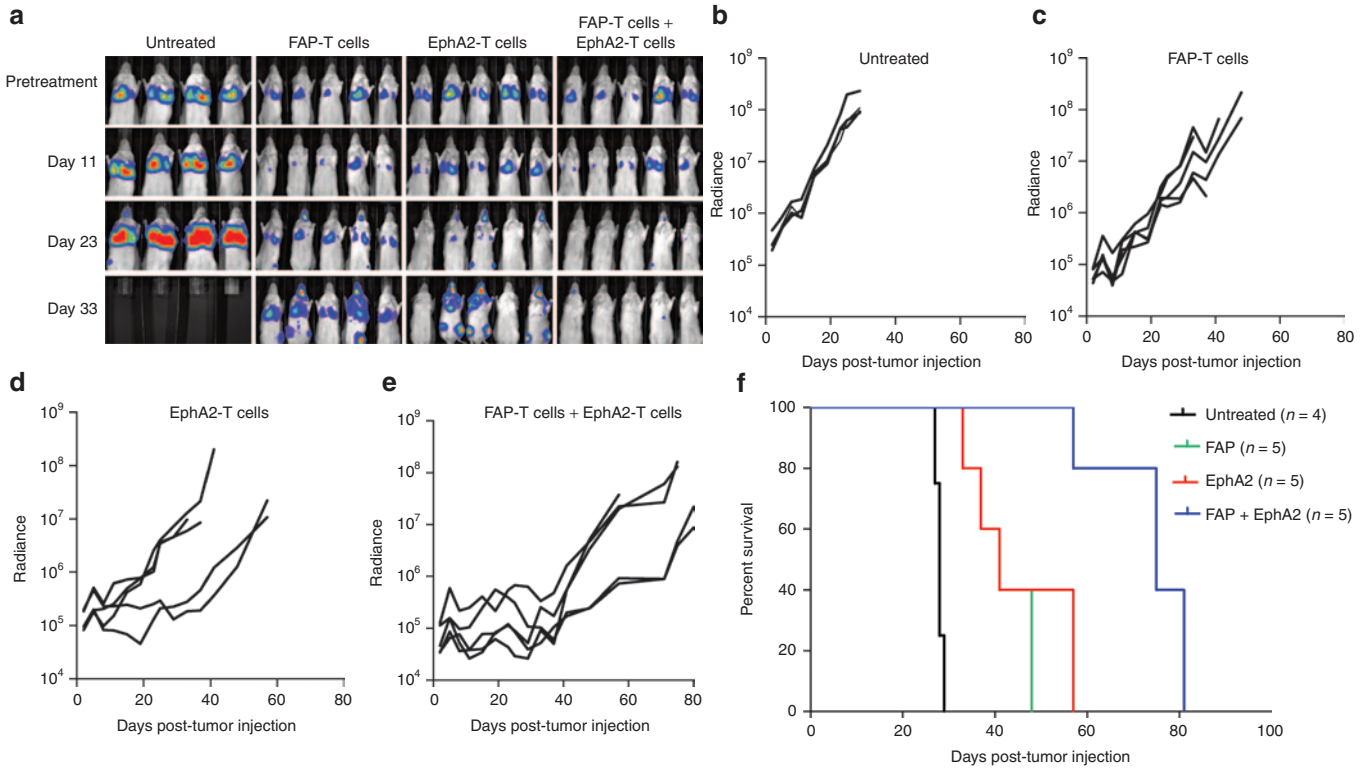

Figure 7 Co-targeting CAFs and cancer cells results in an enhanced antitumor response and improved survival. (**a**) A549.eGFP.FFLuc cells were injected i.v. on day 0. On day 7, mice received an i.v. administration of FAP-T cells (or) EphA2-T cells, (or) FAP-T cells and EphA2-T cells. All groups received an i.p. injection of 1,500 U IL-2. Treatment was repeated two more times a week apart. Untreated mice served as controls. Tumor progression was followed by *in vivo* bioluminescence imaging. Images of representative animals are shown. (**b–e**) Solid lines represent each individual mouse (**f**) Kaplan–Meier survival curve of untreated mice ($n = 4$) or those treated with FAP-T cells ($n = 5$) or EphA2-T cells ($n = 5$), or FAP and EphA2-T cells ($n = 5$).

and analyzed for the expression of EphA2. All tested tumors ($n = 6$) were EphA2 positive, excluding antigen loss as a potential explanation (**Supplementary Figure S10**).

DISCUSSION

Here we describe the development and characterization of a novel CAR specific for FAP, and show that T cells expressing this CAR can effectively target human and murine FAP-positive cells. These FAP-specific T cells produce immunostimulatory cytokines and induce tumor cytolysis when co-cultured with FAP-positive targets. The FAP-specific T cells also targeted murine FAP-positive cancer-associated fibroblasts in a human-tumor xenograft model diminishing the growth of FAP-negative tumors. Finally, the combined targeting of FAP-positive cancer-associated fibroblasts and the tumor-associated antigen EphA2 on the tumor cells themselves enhances the antitumor activity of either component alone.

The tumor microenvironment is a complex milieu with heterogeneous components and is no longer considered an innocent bystander in cancer development.[22] Instead, it plays an essential role in tumor initiation, progression,[23] and mediates therapeutic resistance.[24] Targeting these auxiliary cells in addition to the cancer cells may therefore increase the effectiveness of cancer-targeted therapies.[25] FAP-positive cancer-associated fibroblasts are the central cellular component of the tumor stroma and make a critical contribution to immunosupression,[12] stromagenesis, vascularization, and extracellular matrix remodeling.[26] These effects have been validated in preclinical studies, in which targeting of FAP with a monoclonal FAP antibody conjugated to maytansinoid, disrupted fibroblastic and vascular structures with a concomitant decrease in tumor growth and minimal side-effects.[27] Unfortunately, however, infusion of FAP-specific monoclonal antibody in a phase 2 clinical trial showed no objective tumor response.[28] Similarly, phase 2 clinical trials with small molecule inhibitors such as PT-100 that target all members of the prolyl-peptidase family including FAP failed to show clinical benefit.[29] Immunotherapy using vaccines against FAP has been combined with chemo- or other tumor directed therapies,[13,30,31] but this approach has yet to be evaluated in the clinic, and there is concern about the low objective response rate of cancer vaccines in general.[32] Thus, new immunotherapy approaches are needed to target FAP-positive cancer-associated fibroblasts.

The adoptive transfer of T cells engineered to express CARs has shown encouraging antitumor activity, especially for treating CD19-positive hematological malignancies.[33–36] While CAR-T cells have been less widely used to treat solid tumors, recent clinical trials provide evidence for efficacy, with sustained remissions obtained in patients with active disease.[37,38] The adoptive transfer of FAP-specific CAR-T cells is therefore a promising approach to target FAP-positive cancer-associated fibroblasts in the tumor microenvironment. Moreover, the FAP-specific T cells, we used,

can recognize and kill both human and murine FAP-positive targets with similar affinity, due to the cross-reactivity of the FAP-specific scFV CAR.[39] This allowed us to evaluate the effects of targeting the (murine) tumor stroma within and around the (human) tumor xenograft in an immunodeficient mouse model. We used this FAP-CAR in two different tumor models: the loco-regional B-cell lymphoma model was used to test the role of FAP-positive stroma during tumor initiation, while the non-small cell lung carcinoma xenograft model was used to explore the systemic effects of FAP-specific T cells on established tumor. In the first model, (human) LCLs efficiently induced a reactive (murine) FAP-positive stroma subcutaneously. If LCLs were co-injected with FAP-specific T cells, tumor growth was significantly decreased when compared to control T cells. This effect was a result of targeting murine FAP in the tumor stroma, since T cells restricted in specificity for human FAP had no antitumor activity. In the systemic model, FAP-negative A549 cells induced FAP-positive stroma in the lungs of injected mice, an effect that was diminished by administration of FAP-specific T cells with a resultant decrease in tumor growth and improved survival, with no toxicity or negative effects on wound healing. Recent evidence indicates that FAP expression may not be unique to tumor stroma and may be present on malignant cells themselves.[40–42] Although we confirmed these findings in several other cancer cell lines by using qRT-PCR and FACS analysis, the same assays failed to detect FAP expression in any of the lines used in the *in vivo* models we describe, and so the antitumor effects of FAP-specific T cells cannot be attributed to a direct effect on cancer cells. Instead, gene expression analysis of the lungs of tumor-bearing mice treated with FAP-specific T cells showed upregulation of murine genes involved in innate immune pathways (*e.g.* chemokine and toll-like receptor signaling pathways). Additionally, downregulation of genes such as IL-6 suggests that targeting FAP-positive stroma could potentially staunch the supply of soluble factors required for tumor growth.[19] Hence, destruction of FAP-positive stroma may alleviate the immunosuppressive microenvironment and allow infiltration of immune cells, which indirectly mediate antitumor effects. Further mechanistic analysis awaits the development of a suitable immunocompetent mouse model.

More interestingly, our results also show that co-targeting the tumor directly (tumor cells) and indirectly (FAP-positive stroma) enhances the overall antitumor activity. To target A549 cancer cells, we used EphA2-specific T cells that recognize EphA2 expressed on A549 cells. While expression of EphA2 has been observed on the tumor vasculature of several tumors,[43] qRT-PCR amplification revealed no induction of murine EphA2 in the A549 model used (**Supplementary Figure S11**). Injection of either EphA2- or FAP-specific T cells on day 7 post tumor injection improved survival over control animals (indicating that stroma targeting alone can be as effective as targeting a tumor antigen) but co-injection of FAP-specific and EphA2-specific T cells was better still. Using murine systems expressing model antigens, investigators have shown that consistent eradication of solid tumors requires the destruction of both stroma and cancer cells.[44] The current data extend these findings to human tumors expressing clinically relevant human tumor and stromal antigens. Long-term follow-up of the animals showed tumor recurrence, even though the regrowing tumors continued to express the targeted antigens. FAP-specific T cells only persisted for up to one week post infusion and it is likely that this limited T-cell persistence coupled with the highly aggressive tumor model accounted for the recurrences observed.

In conclusion, our findings provide preclinical evidence for the therapeutic potential of FAP-specific T cells. These T cells destroy FAP-positive stroma and have antitumor activity *in vivo*. When co-administered with tumor-specific T cells, FAP-specific T cells enhance their antitumor activity *in vivo*. Thus, targeting FAP with FAP-specific T cells either alone or as an adjuvant therapy has the potential to improve current immunotherapeutic approaches for cancer.

MATERIALS AND METHODS

Tumor cell lines. The non-small cell lung cancer cell lines NCI-H1299 and A549, chronic myelogenous leukemia cell line K562, metastatic lung fibroblast line Hs894, glioblastoma line U87, and pancreatic cancer cell line PL45 were purchased from the American Type Culture Collection (ATCC; Manassas, Virginia). HPS-19I was provided by Dr. David Rowley, coauthor. C666.1 was provided by Dr. Nancy Raab-Traub, University of North Carolina, Chapel Hill, NC. LCLs were generated as previously described.[45] The 'Characterized Cell Line Core Facility' at MD Anderson Cancer Center, Houston, Texas, performed cell line validation. For the procedures on the generation of genetically modified cell lines, see **Supplementary Materials and Methods**.

Generation of an FAP-specific CAR. The mhFAP -cross reactive single chain variable fragment (scFv MO36) was previously generated by phage display from an immunized FAP/ knock-out mouse.[39] This scFV (designated mhFAP) was subcloned into an SFG retroviral vector containing the human IgG1-CH2CH3 domain, a CD28 transmembrane domain, and costimulatory domains derived from CD28 and the CD3 ζ-chain.[46] The cloning of the FAP-specific CAR was verified by sequencing (Seqwright, Houston, Texas). The PSCA-specific CAR was kindly provided by Dr. Juan Vera, Center for Cell and Gene Therapy, Baylor College of Medicine, Houston, Texas.

Retrovirus production and transduction of T cells. CAR expressing T cells were generated as previously described.[21] Briefly, PBMCs, obtained from healthy donors in accordance to protocols approved by the Institutional Review Board of Baylor College of Medicine, were stimulated on OKT3 (Ortho Biotech, Bridgewater, New Jersey) and CD28 (Becton Dickinson, Mountain View, California) antibodies-coated non-tissue culture treated 24-well plates. Human interleukin-2 (IL-2; Proleukin; Chiron, Emeryville, California) was added to cultures on day 2, and on day 3 T cells were transduced with the retroviral particles on RetroNectin® (Clontech, Mountain View, California) coated plates in the presence IL-2. T cells were subsequently expanded with IL-2. NT-T cells, used as controls, were activated with OKT3/CD28 and expanded in parallel with IL-2.

Flow cytometry. For immunophenotyping, cells were stained with fluorescein-conjugated monoclonal antibodies (Becton Dickinson, San Jose, California) directed against CD4, CD8, and CD56 surface proteins. Isotype controls were immunoglobulin G1–fluorescein isothiocyanate (IgG1-FITC; BD), IgG1–phycoerythrin (IgG1-PE; BD), IgG1–peridinin chlorophyll protein (IgG1-PerCP; BD), and isotype Cy5 (Jackson ImmunoResearch Laboratories, West Grove, Philadelphia). The surface expression of CAR on T cells was analyzed using a CH2CH3 Cy5 antibody (Jackson ImmunoResearch Laboratories). For each sample, 10,000 cells were analyzed by FACSCalibur instrument (BD, Becton Dickinson, Mountain View, California) with the Cell Quest Software (Becton Dickinson) or with FCS Express software (De Novo Software, Los Angeles, California). FAP-positive cells were stained using the sheep polyclonal

anti-FAP (R&D Systems, Inc., Minneapolis, Minnesota) for 1 hour followed by donkey anti-sheep IgG (H+L)-PerCP for 30 minutes (R&D Systems) for tumor samples, and Northern Lights Anti-Sheep IgG-NL 557 for 1 hour (R&D Systems) for cell lines.

Ex vivo *functional analysis of T cells.* NT- and CAR-T cells were plated at 2:1 ratio with tumor cells. Cytokine release after 24 hours of culture was measured using the 13-plex Milliplex MAP (EMD Millipore, Billerica, Massachusetts). Standard chromium (^{51}Cr) release assays were performed as previously described.[47]

Loco-regional LCL tumor model. All animal experiments followed a protocol approved by the Baylor College of Medicine Institutional Animal Care and Use Committee. Institute for Cancer Research (ICR)-SCID mice were purchased from Taconic (IcrTac:ICR-Prkdcscid; Fox Chase C.B-17 SCID™ ICR; Taconic, Hudson, New York). Male 8- to 12-week-old mice were sublethally irradiated (230 cGy) 48 hours prior to tumor challenge. An admixture of 5×10^6 LCL.eGFP.ffLuc cells with either 10×10^6 NT-control T cells or 10×10^6 FAP-specific T cells in PBS were administered subcutaneously in to the flank region. rhIL-2 (1,500 U) was administered intraperitoneally. Isofluorane anesthetized animals were imaged using the IVIS® system (IVIS, Xenogen Corp., Alameda, California) 10 to 15 minutes after 150 mg/kg D-luciferin (Xenogen) was injected per mouse intraperitoneally. The photons emitted from the luciferase-expressing tumor cells were quantified using Living Image software (Caliper Life Sciences, Hopkinton, Massachusetts). A constant region-of-interest was drawn over the tumor region and the intensity of the signal measured as total photon/second/cm^2/steradian (p/s/cm^2/sr). Animals were initially imaged every two days, and once a week thereafter. Mice were euthanized when tumors became necrotic or when they met euthanasia criteria (weight loss, signs of distress) in accordance with the Center for Comparative Medicine at Baylor College of Medicine.

Systemic A549 tumor model. All animal experiments followed a protocol approved by the Baylor College of Medicine Institutional Animal Care and Use Committee. Around 9- to 12-week-old SCID Beige mice were purchased from Charles River (CB17.Cg-PrkdcscidLystbg/Crl; Fox Chase SCID® Beige mouse; Charles River Laboratories International, Inc., Wilmington, Massachusetts). 2.5×10^6 A549.eGFP.ffLuc cells in PBS were injected intravenously on day 0. To determine the efficacy of targeting FAP-positive murine stroma, mice were treated with an intravenously administration of either 10×10^6 NT-T cells or 10×10^6 FAP-specific T cells on day 4-post tumor challenge. Untreated animals served as controls. rhIL-2 (1,500 U) was administered intraperitoneally in all the groups. To determine the efficacy of co-targeting cancer-associated fibroblasts and cancer cells, mice were treated on day 7 post tumor challenge with either 10×10^6 FAP-specific T cells or 10×10^6 EphA2-specific T cells or 5×10^6 FAP-specific T cells and 5×10^6 EphA2-specific T cells. Untreated animals served as controls. rhIL-2 (1,500 U) was administered intraperitoneally in all the groups. Animals were imaged as described.

Quantitative real time PCR. RNA was extracted from cell lines using the RNeasy Mini Kit (Qiagen, Valencia, California). The RNeasy Lipid Tissue Mini Kit (Qiagen) was used to extract RNA from excised tumors. Relative quantification of FAP mRNA expression was done using TaqMan® One-Step RT-PCR Master Mix Reagents (Applied Biosystems, Branchburg, New Jersey) using the primer/probes for murine FAP, human FAP, murine beta actin, and human beta actin (all from Applied Biosystems).

Gene expression array analysis. About 2.5×10^6 A549.eGFP.FFLuc cells were injected intravenously into SCID-Beige mice on day 0. On day 4 mice were treated intravenously with 10×10^6 NT- or FAP-T cells along with 1,500 U IL-2 administered intraperitoneally. Lungs were excised 48 hours post T-cell injection and total RNA was isolated using RNeasy Lipid Tissue Mini Kit (Qiagen). Transcriptional profiling was performed using GeneChip Mouse Gene 1.0 ST Array (Affymetrix, Santa Clara, California.). Arrays of tumors treated with NT- or FAP-T cells were performed as triplicates using six lung samples in each group. Data preprocessing and summarization were performed using Robust Multichip Average. Statistical tests of differential expression were conducted using the moderated paired *t*-test. The Benjamini–Hochberg multiple testing adjustment was applied in order to control the false discovery rate. Genes present at significantly different ($P < 0.05$; fold change ≥ 1.5) levels in tumor bearing lungs treated FAP-specific or NT-T cells were submitted to IPA software (Ingenuity Systems, Redwood, California) and analyzed to uncover gene pathways that were overrepresented in the dataset. Both transcriptional profiling and analysis of microarray data were performed by Genome explorations USA (Memphis, Tennessee).

Statistical analysis. All *in vitro* experiments were performed either in triplicate, quadruplicate, or in pentuplicate. GraphPad Prism 5 software (GraphPad software, Inc., La Jolla, California) was used for statistical analysis. Measurement data were presented as mean ± standard deviation (SD). The differences between means were tested by nonparametric Mann–Whitney U test. The significance level used was $P < 0.05$. For the mouse experiments, tumor radiance data were log-transformed and summarized using mean ± SD at baseline and multiple subsequent time points for each group of mice. Fold changes in tumor radiance from baseline at each time point were calculated and compared between groups using one-way Anova. Survival determined from the time of tumor cell injection was analyzed by the Kaplan–Meier method and by the log-rank test.

SUPPLEMENTARY MATERIAL

Figure S1. FAP-specific T cells secrete variable amounts of proinflammatory cytokines.
Figure S2. Reactive stroma is induced in LCL xenografts.
Figure S3. T cells specific for human FAP (hFAP) recognize and kill hFAP-positive targets.
Figure S4. hFAP-specific T cells have no antitumor activity *in vivo*.
Figure S5. mFAP is induced in A549 lung cancer xenografts.
Figure S6. hFAP-specific T cells have no antitumor activity in A549 systemic model.
Figure S7. FAP-specific T cells expand and persist only in the presence of a tumor.
Figure S8. Treatment with FAP-specific T cells does not induce acute organ damage or affect wound healing.
Figure S9. EphA2-specific T cells recognize and kill human FAP-positive targets.
Figure S10. Recurrent tumors continue to express target antigen.
Figure S11. Murine EphA2 expression is not induced in A549 lung cancer xenografts.
Table S1. Differentially expressed genes in lungs of tumor-bearing mice treated with FAP-specific or NT-T cells.
Materials and Methods.

ACKNOWLEDGMENTS

We thank Cliona M. Rooney for helpful discussions and advice. We also thank LaTerrica Williams, Troung Dang and Steven Ressler for their help. K.K.H.C. is a Melnick scholar and was supported by NIH grants 5T32HL092332 and 5T32GM007330. This work was supported by NIH grants 1R01CA148748-01A1 and P01CA94237, and by the Adrienne Helis Malvin Medical Research Foundation through its direct engagement in the continuous active conduct of medical research in conjunction with Baylor College of Medicine and the Adoptive T-cell Therapy for Lung Cancer Program. The Characterized Cell Line Core Facility at MD Anderson Cancer Center is funded by NCI # CA16672. The Center for Cell and Gene Therapy has a research collaboration with Celgene and bluebird bio. S.K., K.K.H.C., D.R.S., X.T.S., K.P., and S.G. have patent applications in the field of T-cell and gene-modified T-cell therapy for cancer.

REFERENCES

1. Dvorak, HF (1986). Tumors: wounds that do not heal. Similarities between tumor stroma generation and wound healing. *N Engl J Med* **315**: 1650–1659.
2. Hanahan, D and Weinberg, RA (2011). Hallmarks of cancer: the next generation. *Cell* **144**: 646–674.
3. Räsänen, K and Vaheri, A (2010). Activation of fibroblasts in cancer stroma. *Exp Cell Res* **316**: 2713–2722.
4. Heldin, CH, Rubin, K, Pietras, K and Ostman, A (2004). High interstitial fluid pressure - an obstacle in cancer therapy. *Nat Rev Cancer* **4**: 806–813.
5. Cukierman, E and Bassi, DE (2012). The mesenchymal tumor microenvironment: a drug-resistant niche. *Cell Adh Migr* **6**: 285–296.
6. Tlsty, TD and Hein, PW (2001). Know thy neighbor: stromal cells can contribute oncogenic signals. *Curr Opin Genet Dev* **11**: 54–59.
7. Bhowmick, NA, Neilson, EG and Moses, HL (2004). Stromal fibroblasts in cancer initiation and progression. *Nature* **432**: 332–337.
8. Elenbaas, B and Weinberg, RA (2001). Heterotypic signaling between epithelial tumor cells and fibroblasts in carcinoma formation. *Exp Cell Res* **264**: 169–184.
9. Rettig, WJ, Garin-Chesa, P, Beresford, HR, Oettgen, HF, Melamed, MR and Old, LJ (1988). Cell-surface glycoproteins of human sarcomas: differential expression in normal and malignant tissues and cultured cells. *Proc Natl Acad Sci USA* **85**: 3110–3114.
10. Garin-Chesa, P, Old, LJ and Rettig, WJ (1990). Cell surface glycoprotein of reactive stromal fibroblasts as a potential antibody target in human epithelial cancers. *Proc Natl Acad Sci USA* **87**: 7235–7239.
11. Saadi, A, Shannon, NB, Lao-Sirieix, P, O'Donovan, M, Walker, E, Clemons, NJ *et al.* (2010). Stromal genes discriminate preinvasive from invasive disease, predict outcome, and highlight inflammatory pathways in digestive cancers. *Proc Natl Acad Sci USA* **107**: 2177–2182.
12. Kraman, M, Bambrough, PJ, Arnold, JN, Roberts, EW, Magiera, L, Jones, JO *et al.* (2010). Suppression of antitumor immunity by stromal cells expressing fibroblast activation protein-alpha. *Science* **330**: 827–830.
13. Loeffler, M, Krüger, JA, Niethammer, AG and Reisfeld, RA (2006). Targeting tumor-associated fibroblasts improves cancer chemotherapy by increasing intratumoral drug uptake. *J Clin Invest* **116**: 1955–1962.
14. Lee, PP, Yee, C, Savage, PA, Fong, L, Brockstedt, D, Weber, JS *et al.* (1999). Characterization of circulating T cells specific for tumor-associated antigens in melanoma patients. *Nat Med* **5**: 677–685.
15. Vera, J, Savoldo, B, Vigouroux, S, Biagi, E, Pule, M, Rossig, C *et al.* (2006). T lymphocytes redirected against the kappa light chain of human immunoglobulin efficiently kill mature B lymphocyte-derived malignant cells. *Blood* **108**: 3890–3897.
16. Tuxhorn, JA, Ayala, GE, Smith, MJ, Smith, VC, Dang, TD and Rowley, DR (2002). Reactive stroma in human prostate cancer: induction of myofibroblast phenotype and extracellular matrix remodeling. *Clin Cancer Res* **8**: 2912–2923.
17. Katari, UL, Keirnan, JM, Worth, AC, Hodges, SE, Leen, AM, Fisher, WE *et al.* (2011). Engineered T cells for pancreatic cancer treatment. *HPB (Oxford)* **13**: 643–650.
18. Foster, AE, Dotti, G, Lu, A, Khalil, M, Brenner, MK, Heslop, HE *et al.* (2008). Antitumor activity of EBV-specific T lymphocytes transduced with a dominant negative TGF-beta receptor. *J Immunother* **31**: 500–505.
19. Vicent, S, Sayles, LC, Vaka, D, Khatri, P, Gevaert, O, Chen, R *et al.* (2012). Cross-species functional analysis of cancer-associated fibroblasts identifies a critical role for CLCF1 and IL-6 in non-small cell lung cancer in vivo. *Cancer Res* **72**: 5744–5756.
20. Kinch, MS, Moore, MB and Harpole, DH Jr (2003). Predictive value of the EphA2 receptor tyrosine kinase in lung cancer recurrence and survival. *Clin Cancer Res* **9**: 613–618.
21. Chow, KK, Naik, S, Kakarla, S, Brawley, VS, Shaffer, DR, Yi, Z *et al.* (2013). T cells redirected to EphA2 for the immunotherapy of glioblastoma. *Mol Ther* **21**: 629–637.
22. Marx, J (2008). Cancer biology. All in the stroma: cancer's Cosa Nostra. *Science* **320**: 38–41.
23. Polyak, K, Haviv, I and Campbell, IG (2009). Co-evolution of tumor cells and their microenvironment. *Trends Genet* **25**: 30–38.
24. Chometon, G and Jendrossek, V (2009). Targeting the tumour stroma to increase efficacy of chemo- and radiotherapy. *Clin Transl Oncol* **11**: 75–81.
25. Zhang, B, Bowerman, NA, Salama, JK, Schmidt, H, Spiotto, MT, Schietinger, A *et al.* (2007). Induced sensitization of tumor stroma leads to eradication of established cancer by T cells. *J Exp Med* **204**: 49–55.
26. Santos, AM, Jung, J, Aziz, N, Kissil, JL and Puré, E (2009). Targeting fibroblast activation protein inhibits tumor stromagenesis and growth in mice. *J Clin Invest* **119**: 3613–3625.
27. Ostermann, E, Garin-Chesa, P, Heider, KH, Kalat, M, Lamche, H, Puri, C *et al.* (2008). Effective immunoconjugate therapy in cancer models targeting a serine protease of tumor fibroblasts. *Clin Cancer Res* **14**: 4584–4592.
28. Hofheinz, RD, al-Batran, SE, Hartmann, F, Hartung, G, Jäger, D, Renner, C *et al.* (2003). Stromal antigen targeting by a humanised monoclonal antibody: an early phase II trial of sibrotuzumab in patients with metastatic colorectal cancer. *Onkologie* **26**: 44–48.
29. Cunningham, CC (2007). Talabostat. *Expert Opin Investig Drugs* **16**: 1459–1465.
30. Lee, J, Fassnacht, M, Nair, S, Boczkowski, D and Gilboa, E (2005). Tumor immunotherapy targeting fibroblast activation protein, a product expressed in tumor-associated fibroblasts. *Cancer Res* **65**: 11156–11163.
31. Wen, Y, Wang, CT, Ma, TT, Li, ZY, Zhou, LN, Mu, B *et al.* (2010). Immunotherapy targeting fibroblast activation protein inhibits tumor growth and increases survival in a murine colon cancer model. *Cancer Sci* **101**: 2325–2332.
32. Klebanoff, CA, Acquavella, N, Yu, Z and Restifo, NP (2011). Therapeutic cancer vaccines: are we there yet? *Immunol Rev* **239**: 27–44.
33. Savoldo, B, Ramos, CA, Liu, E, Mims, MP, Keating, MJ, Carrum, G *et al.* (2011). CD28 costimulation improves expansion and persistence of chimeric antigen receptor-modified T cells in lymphoma patients. *J Clin Invest* **121**: 1822–1826.
34. Porter, DL, Levine, BL, Kalos, M, Bagg, A and June, CH (2011). Chimeric antigen receptor-modified T cells in chronic lymphoid leukemia. *N Engl J Med* **365**: 725–733.
35. Brentjens, RJ, Rivière, I, Park, JH, Davila, ML, Wang, X, Stefanski, J *et al.* (2011). Safety and persistence of adoptively transferred autologous CD19-targeted T cells in patients with relapsed or chemotherapy refractory B-cell leukemias. *Blood* **118**: 4817–4828.
36. Kochenderfer, JN, Dudley, ME, Feldman, SA, Wilson, WH, Spaner, DE, Maric, I *et al.* (2012). B-cell depletion and remissions of malignancy along with cytokine-associated toxicity in a clinical trial of anti-CD19 chimeric-antigen-receptor-transduced T cells. *Blood* **119**: 2709–2720.
37. Louis, CU, Savoldo, B, Dotti, G, Pule, M, Yvon, E, Myers, GD *et al.* (2011). Antitumor activity and long-term fate of chimeric antigen receptor-positive T cells in patients with neuroblastoma. *Blood* **118**: 6050–6056.
38. Park, JR, Digiusto, DL, Slovak, M, Wright, C, Naranjo, A, Wagner, J *et al.* (2007). Adoptive transfer of chimeric antigen receptor re-directed cytolytic T lymphocyte clones in patients with neuroblastoma. *Mol Ther* **15**: 825–833.
39. Brocks, B, Garin-Chesa, P, Behrle, E, Park, JE, Rettig, WJ, Pfizenmaier, K *et al.* (2001). Species-crossreactive scFv against the tumor stroma marker "fibroblast activation protein" selected by phage display from an immunized FAP-/- knock-out mouse. *Mol Med* **7**: 461–469.
40. Shi, M, Yu, DH, Chen, Y, Zhao, CY, Zhang, J, Liu, QH *et al.* (2012). Expression of fibroblast activation protein in human pancreatic adenocarcinoma and its clinicopathological significance. *World J Gastroenterol* **18**: 840–846.
41. Mentlein, R, Hattermann, K, Hemion, C, Jungbluth, AA and Held-Feindt, J (2011). Expression and role of the cell surface protease seprase/fibroblast activation protein-a (FAP-a) in astroglial tumors. *Biol Chem* **392**: 199–207.
42. Goscinski, MA, Suo, Z, Flørenes, VA, Vlatkovic, L, Nesland, JM and Giercksky, KE (2008). FAP-alpha and uPA show different expression patterns in premalignant and malignant esophageal lesions. *Ultrastruct Pathol* **32**: 89–96.
43. Ogawa, K, Pasqualini, R, Lindberg, RA, Kain, R, Freeman, AL and Pasquale, EB (2000). The ephrin-A1 ligand and its receptor, EphA2, are expressed during tumor neovascularization. *Oncogene* **19**: 6043–6052.
44. Spiotto, MT, Rowley, DA and Schreiber, H (2004). Bystander elimination of antigen loss variants in established tumors. *Nat Med* **10**: 294–298.
45. Rooney, CM, Smith, CA, Ng, CY, Loftin, SK, Sixbey, JW, Gan, Y *et al.* (1998). Infusion of cytotoxic T cells for the prevention and treatment of Epstein-Barr virus-induced lymphoma in allogeneic transplant recipients. *Blood* **92**: 1549–1555.
46. Pulè, MA, Straathof, KC, Dotti, G, Heslop, HE, Rooney, CM and Brenner, MK (2005). A chimeric T cell antigen receptor that augments cytokine release and supports clonal expansion of primary human T cells. *Mol Ther* **12**: 933–941.
47. Gottschalk, S, Edwards, OL, Sili, U, Huls, MH, Goltsova, T, Davis, AR *et al.* (2003). Generating CTLs against the subdominant Epstein-Barr virus LMP1 antigen for the adoptive immunotherapy of EBV-associated malignancies. *Blood* **101**: 1905–1912.